arXiv:1512.01695v1 [astro-ph.HE] 5 Dec 2015

Statistical Analysis of the Parameters of Gamma-Ray Bursts with Known Redshifts and Peaked Optical Light Curves

Beskin G.[1,2], Oganesyan G.[3], Greco G.[4] and Karpov S.[1,2]

[1]Special Astrophysical Observatory of the Russian AS, Nizhnij Arkhyz, 369167 Russia; beskin@sao.ru
[2]Kazan Federal University,Kazan, 420008 Russia
[3]Southern Federal University, Rostov-on-Don, 344000 Russia
[4]University of Urbino, Urbino, 61029 Italy

Abstract

We present the statistical analysis of the properties of gamma-ray bursts with measured host galaxy redshifts and peaked optical light curves in proper frames of reference. The optical transients are classified by comparing the time lag of the optical peak relative to the GRB trigger with the duration of the gamma-ray emission itself. The results of the correlation analysis of all possible pairs of energy, spectral, and temporal characteristics of both gamma-ray and optical emissions are given. We specify the pairs of the parameters with correlation coefficients greater than 50% at significance levels better than 1%. The following empirical relations, obtained for the first time, are specifically discussed: a correlation between the peak optical afterglow R band luminosity and redshift $L_R \propto (z+1)^{5.39\pm0.74}$ and a correlation between the peak luminosity of the prompt optical emissions and the time of the peak $L_R \propto T_{\rm peak}^{-3.85\pm1.22}$. We also analyze the similarity of the relationships between the peak optical luminosity and the isotropic equivalent of the total energy of gamma-ray bursts for afterglows ($L_R \propto E_{\rm iso}^{1.06\pm0.22}$) and for prompt optical emissions ($L_R \propto E_{\rm iso}^{1.59\pm0.21}$).

1 INTRODUCTION

Gamma-ray bursts (GRB) are the brightest transient phenomena in the Universe (the isotropic equivalent of their total energy reaches 10^{54} erg). Along with actual bursts, variable sources related to them are also observed in different ranges: radio, infrared, optical, and x-ray. They are less intensive but powerful enough, with luminosities reaching 10^{51} erg s^{-1}. A division of all these manifestations into two types of transients is generally accepted: emission synchronous with gamma-ray (prompt), continuing at least until T_{90} (the time till which 90% of the gamma-ray burst energy is released), and the afterglows, usually starting after the burst turns off. The most popular description of their population is a model which combines the inner and outer shock waves produced while the fragments of the relativistic outflow decelerate due to the collisions inside of it (prompt) and while it decelerates in the outer interstellar medium (afterglow) [1, 2].

Most of the studies are devoted to examining the properties of individual gamma-ray bursts and to attempts of verification of phenomenon models in general. As time has shown, in this approach its self-consistent physical picture is far from being constructed, especially for the optical components of the bursts. It is still unclear whether there occur reverse shock waves, what energy structure does a relativistic jet have, what is the density distribution in the ambient interstellar medium surrounding the burst, etc. In these circumstances, the search for statistical relationships between various parameters of bursts in their subsamples formed according to various criteria and with the minimal use of model

representations remains a topical task. In its context, a particularly important role has the analysis of the properties of the sample of gamma-ray bursts with measured redshifts, numbering about 250 objects [3]. This amount of data allows us to perform a statistical analysis of the parameters of gamma-ray bursts in the proper frame of reference, revealing empirical relations between intrinsic physical characteristics [4, 5, 6, 7, 8, 9, 10]. At the same time, similar relations are also analyzed for the optical components of the bursts [11, 12, 13, 14, 15, 16], the host galaxies [17, 18], and the characteristics of the local interstellar medium in the GRB progenitors [19].

The main problem of all such studies is to find an optimum ratio between the object selection criteria and the sample size: the latter decreases for a more rigorous selection, and subsequently the significance of established statistical dependences falls, while the role of selection effects increases. We study the correlations between the parameters of GRBs with measured redshifts and peaked optical light curves. The latter condition isolates a specific physical condition within any given model: deceleration of either the ejecta colliding inside the jet in the case of prompt optical emissions or the ejected matter in the outer interstellar medium. Notice that it is not known in advance which kind of physical processes would determine the occurrence of this peak. The division of objects into subsamples was carried out by comparing the time interval between the beginning of the optical brightness increase and the time of the trigger with the duration of the gamma-ray emission itself (prompt optical emissions, afterglows, and afterglows accompanied by residual gamma-ray radiation), while the identification of the physical type of optical emissions (prompt or afterglow) stems from the statistical analysis of the entire subsample. This way, some objects, initially classified as the prompt optical emissions were subsequently found to be close to the afterglows by their statistical properties. Notice that the use of a sample of GRBs with known redshifts for the statistical analysis allows us to pose the problem of the cosmological evolution of the properties of both the bursts themselves and the interstellar medium in the region of their localization. Section 2 of this paper gives the definitions and techniques of obtaining different characteristics of the objects, and describes the methods of statistical analysis of the initial data and the obtained results. Sections 3, 4, 5 discuss some of the most important correlations between the GRB parameters we found: the relationship between the optical luminosity at the light curve peaks and the redshift, between the optical luminosity and the burst energy in the gamma-ray range, and between the luminosity and the time of the peak. Section 6 briefly summarizes the results obtained.

2 THE GRB SAMPLE

Fifty-four gamma-ray bursts with known redshifts and peaked optical light curves were selected for the analysis. The time dependences of the detected radiation flux both in the gamma-ray and optical (in stellar magnitudes) ranges served as the data sources for determining GRB parameters. In the latter case, these are, as a rule, the light curves in the R band, $R(t)$, sometimes with modified filters, $r'(t)$, $R_C(t)$, and $r(t)$, in one case in the V band (GRB 050730), and in two cases in the white light (GRB 100906A and GRB 080810). With the use of calibrations from [20], spectral flux densities in the respective F_ν bands in the observer's reference frame were found. The F_ν values were converted into the spectral flux densities F_R at the effective R-band wavelength in the proper frame of reference. If there were no data on the optical spectral index β, $F_\nu \propto \nu^{-\beta}$, the mean value $\beta = 0.75$ [21] for GRB optical components was used, and the following values were determined: the flux in the observer's frame of reference

$$F_{\rm opt} = \int_{\nu_1}^{\nu_2} F_0\, \nu^{-\beta}\, d\nu,$$

where ν_1 and ν_2 are the frequency boundaries of a photometric band in the observer's frame of reference; the integral optical flux $S_{\rm opt}$ (the result of numerical integration of $F_{\rm opt}(t)$ over time); the time of the optical peak relative to the trigger time of a gamma-ray burst $t_{\rm peak}$; the increase and decrease indices

of the optical radiation intensity, $F_{\rm opt} \propto t^{\alpha_r}$, $F_{\rm opt} \propto t^{\alpha_d}$. The parameters of the gamma-ray emission—the peak $F_{\rm iso}$ and integral $S_{\rm iso}$ fluxes in the range of 15–350 keV, the time of the release of 90% of the GRB energy t_{90}, and the spectral index of the energy distribution α—were adopted from Butler et al. [22]. Table 1 lists the data on the gamma-ray bursts and their parameters in the observer's frame of reference. Taking into account the extinction in the Galaxy [23], the brightness of the host galaxy (if available), and the extinction in it, the following GRB parameters were determined for the standard cosmological model with $\Omega_M = 0.3$, $\Omega_\Lambda = 0.7$, $H_0 = 70$ km s^{-1} Mpc^{-1} in the proper frame of reference: the maximal optical R band luminosity

$$L_R = 4\pi D^2 \int\limits_{\nu_{R_0}}^{\nu_{R_1}} F_0\, \nu^{-\beta}\, d\nu, \tag{1}$$

where ν_{R_0} and ν_{R_1} are the frequency boundaries of the standard R band, and D is the photometric distance; the total optical energy E_R for the same range (the time integral of $L_R(t)$); the time-related parameters $T_{\rm peak}$, T_{90} taking into account cosmological contraction. The isotropic equivalent of the gamma-ray burst energy in the extended range of 1–10 000 keV $E_{\rm iso}$ was adopted from [22], the peak luminosity $L_{\rm iso}$ was derived from $F_{\rm iso}$ as

$$L_{\rm iso} = 4\pi D^2 F_{\rm iso}. \tag{2}$$

If the extinction A_R in the host galaxy was not measured, then based on the data on A_V for 76 bursts from [13], we determined the average of these values at a corresponding redshift and transformed them into A_R using the model of extinction in the Magellanic Clouds [24]. The data on the parameters of the gamma-ray bursts in the proper frame of reference are presented in Table 2.

All the optical transients have been classified into one of four following types based on the ratio between the duration of gamma-ray emission itself and the lag of the beginning of the optical brightness increase relative to the time of the trigger.

• P (prompt); thirteen optical transients are classified here whose brightness begins to increase before the attenuation of gamma-ray radiation. This type includes four events, referred to as P?, whose belonging to P is ambiguous; they may belong to the A(U) type (see below).

• A (afterglow); 34 transients whose brightness begins to increase after the gamma-ray activity is ended.

• A(U; seven transients whose brightness is increasing in the presence of underlying residual gamma-ray radiation after 90% of the total burst energy is released.

For the statistical analysis, seven samples were formed containing the following types of objects:

(1) P and P?-type transients;

(2) only afterglows A;

(3) only the transients with underlying continuing gamma-ray activity A(U);

(4) all 54 optical transients;

(5) afterglows A and transients with underlying continuing gamma-ray activity A(U);

(6) only prompt optical emissions P;

(7) the A-type transients along with A(U) and P?.

Unweighted Pearson correlation coefficients R and their significance levels SL were determined between all possible pairs of GRB parameters x and y from these samples by the formulas

$$R(x,y) = \frac{\sum (x_i - \bar{x})(y_i - \bar{y})}{\sqrt{\sum (x_i - \bar{x})^2 \sum (y_i - \bar{y})^2}}, \tag{3}$$

$$\mathrm{SL}(R) = 1 - \frac{2\Gamma\left(\dfrac{n-1}{2}\right)}{\sqrt{\pi}\,\Gamma\left(\dfrac{n-2}{2}\right)} \int\limits_0^R \left(1 - r^2\right)^{\frac{n-4}{2}} dr, \tag{4}$$

where $\bar{x}$ and $\bar{y}$ are the average values of x and y, Γ is the Euler gamma function, n is the number of points (x_i, y_i). Correlations between the parameters with $R > 0.50$ and the significance levels of $\mathrm{SL} < 1\%$ were assumed to be significant, and the linear regression coefficients were then determined for these parameters (Table 3).

3 $L_{\mathrm{opt}} : (z+1)$ CORRELATION

Among all the correlation relationships established in this study, the $L_R : (z+1)$ dependence (Fig. 1), discovered for the first time, in our opinion presents the greatest interest. In particular, its presence leads to the concept of probable cosmological evolution of the local interstellar medium in the gamma-ray burst birthplaces. Notice that this correlation is highly significant for all object types except for the P-type sample objects, which is corroborating evidence that P?-type transients belong to afterglows (A and A(U)-type objects, whose characteristics virtually coincide in the discussed correlation). To be completely confident that the discovered correlation is real, the possible role of selection effects in its occurrence has to be analyzed. Notice that to determine the effect of selection on the parameters of the bursts in the samples of different types, it is first of all necessary to examine the whole set of brightness estimates for optical companions of the bursts at the time of their discovery. To this end, we built the dependences of the observed magnitudes on $(z+1)$ of optical companions at the times of their discovery and the light curve peak (Fig. 2). Based on the data of Figs. 1 and 2, the following conclusions can be formulated. Given a relatively equal luminosity at different redshifts in the proper reference frames, the observed flux should drop quadratically with $(z+1)$, and therewith at maximum redshifts reach the typical detection limit at around 23^{m}, estimated in our sample from the total light curves. This effect would lead to a lack of low-luminosity objects in the proper frame of reference, whose observed brightness is fainter than 23^{m}, and as a consequence, to a luminosity increase with growing redshift. Nevertheless, no regular radiation flux decrease is observed either in the whole set of brightness estimates for optical transients at the moment of their detection or in the peak brightness. On the other hand, both at $z > 4$ and $z < 2$ the brightness of objects varies within close limits from 19^{m}–20^{m} to 13^{m}–14^{m}, by far exceeding the detection limit of 23^{m}. In other words, the selection by brightness is absent in our data.

We compared the correlation coefficients and linear regression parameters for the group of transients from the A + A(U) + P? sample, localized in different redshift ranges (Table 4). It is easy to see that even if we exclude the transients with $z > 4.5$ and $z < 1$, the luminosity increase with increasing redshift remains detectable and significant. Clearly, if we narrow the redshift range, the correlation coefficients decrease, but nevertheless the linear regression parameters for different groups of transients remain the same within their errors; in particular, the exponents are close to 4–5.

Thus, this brief analysis shows that the observed correlation may not be due to the effects of observational selection of optical transients by their brightness.

To determine the statistical significance of the discovered correlation, we generated a sample of 100 000 optical transients normally distributed by L_R with the average $\log L_R = 46$, $\sigma = 2$ in the logarithmic scale [25] (i.e., with luminosities independent of redshift). The extinctions (Galactic and from the host galaxy) were taken to be $0 < A_R < 3$, and the optical spectrum indices $0.2 < \beta < 1.2$. The A_R and β limits were adopted from the observations [13], the distribution was taken to be uniform — the changes of distribution functions had little effect on the result. Redshifts z in the range of $0 < z < 6$ were randomly assigned to the transients. From this general population we randomly selected subsamples of 50 transients each (2000 subsamples) with the observed brightness

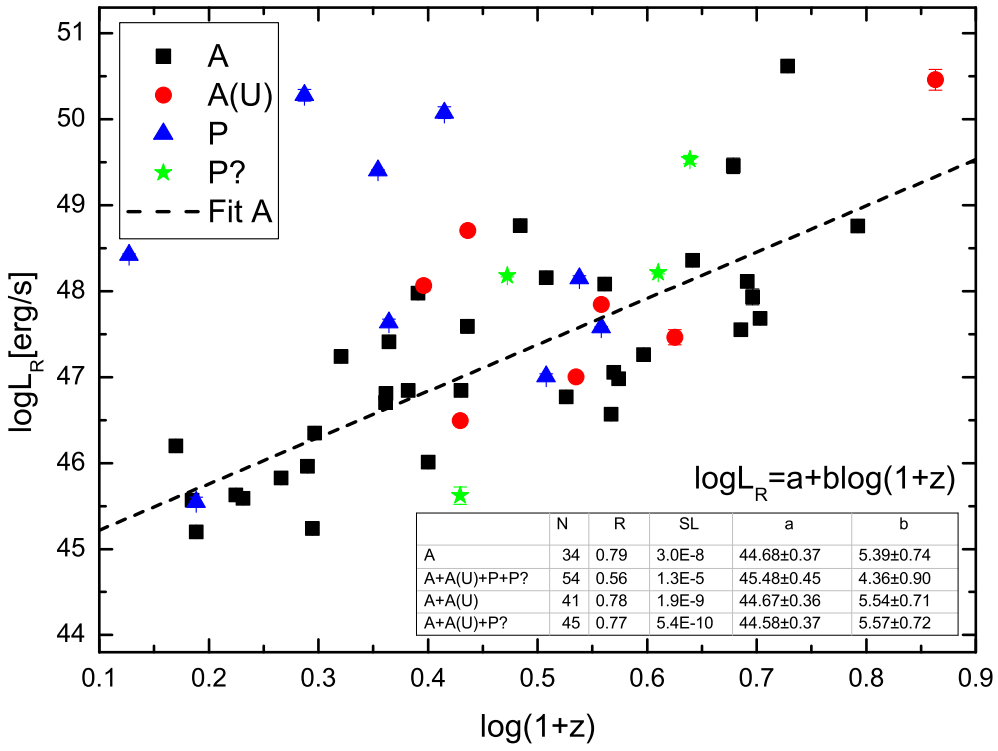

	N	R	SL	a	b
A	34	0.79	3.0E-8	44.68±0.37	5.39±0.74
A+A(U)+P+P?	54	0.56	1.3E-5	45.48±0.45	4.36±0.90
A+A(U)	41	0.78	1.9E-9	44.67±0.36	5.54±0.71
A+A(U)+P?	45	0.77	5.4E-10	44.58±0.37	5.57±0.72

Figure 1: Dependence of the peak optical R band luminosity L_R on redshift z.

exceeding 23^{m}, determined using the luminosity and other above-mentioned parameters. The coefficient of correlation between luminosity and redshift was calculated for each sample. Its value exceeded the 0.7 level only in two cases; in other words, the probability of type I error (of finding a correlation in a random sample of transients when it doesn't exist in the general population) is 10^{-3}. To estimate the probability of error of the second kind, a general population was generated which differed from the previous one by the set law $L_R \propto (1+z)^4$. The correlation coefficient proved to be less than 0.8 in only one sub-sample, which gives the 5×10^{-4} for the probability of type II error (to miss the correlation when it exists in the general population). Ultimately, the luminosity increase in the afterglow light curve peaks with growing GRB redshift appears to be a real effect. It apparently reflects the fact of cosmological evolution of the interstellar medium density in the regions of GRB birth [26]. Indeed, the results of the correlation and regression analysis (see Fig. 1) show that the relation $L_R : (z+1)$ holds for all types of optical transients (samples A, A + A(U), A + A(U) + P?) except for the prompt ones (P) (the correlation substantially decreases when they are added to the afterglows). On the other hand, the P?-type objects can be, with a greater confidence, classified as afterglows, and not as prompt emissions, since the characteristics of the A + A(U) + P? object sample, to which they belong, are virtually identical to those for the afterglow samples A and A + A(U), where they are missing. Moreover, there isAcknowledgements reason to believe that only four (out of nine) brightest cases of prompt optical emissions, which have no relation to the correlation $L_R : (z+1)$, are true prompt emissions whose optical radiation is generated at the stage of internal shock wave collisions near the central engine of the gamma-ray burst, and is not susceptible to the interstellar medium. This is their difference from the remaining five transients of the P sample, whose luminosity–redshift dependence

Table 1: Characteristics of the redshift dependence of the A + A(U) + P? sample peak optical luminosity in different z ranges: the number of transients in the sample N, the Pearson correlation coefficient R, the $\log L_R = a + b\log(z+1)$ linear regression parameters a, b

z	N	R	SL	a	b
all	45	0.77	0.54×10^{-9}	44.58±0.37	5.57±0.72
$z<4.5$	43	0.72	0.65×10^{-7}	44.67±0.40	5.55±0.81
$z>1$	36	0.61	0.84×10^{-4}	45.08±0.62	4.96±1.11
$1<z<4.5$	34	0.50	0.23×10^{-2}	45.39±0.70	4.31±1.30

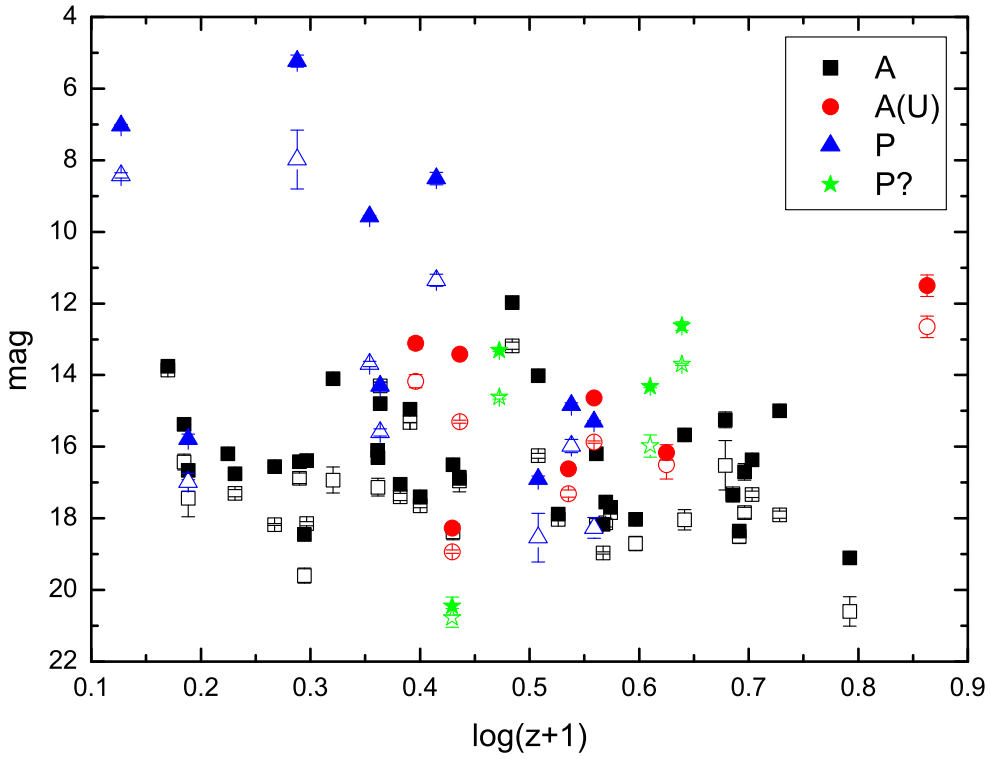

Figure 2: Observed magnitudes of the optical transients (in arbitrary filters) at the moments of discovery (empty symbols) and at the peaks of the light curves (filled symbols) depending on redshift z.

is almost identical to that of the afterglows. Thus, we can assume that there is a group of gamma-ray bursts, whose prompt optical emissions, synchronous with gamma-ray emission, are in fact afterglows by their nature, i.e., the result of the interaction of the jet with the local interstellar medium. In other words, this synchronicity by itself is not a sufficient condition to interpret the prompt optical emission within the model of internal shock waves generated in the collisions of individual ejecta in the jet itself. Quite strong correlation of the energy and peak luminosity of GRBs with redshift $E_{\rm iso} : (z+1)$ and $L_{\rm iso} : (z+1)$ (Figs. 3 and 4) in the objects of the same samples gives evidence for this assumption. Naturally, these relationships get stronger if we include in the sample five transients of prompt optical emission, whose correlation and regression properties are virtually identical to those for the afterglows

A + A(U) + P?. Notice that this correlation is remarkably more significant than the weak relationship found for the full sample of GRBs with measured redshifts ($R = 0.44$) [27], usually explained by the selective properties of Swift's main detector (reduction by the observed flux). Finally, let us point out yet another feature of "true" bursts, the brightest events whose characteristics do not depend on redshift: these objects have no peaks in optical afterglows, i.e., their optical brightness decreases quite monotonically after the peak, coinciding with the gamma-ray burst. This behavior can be interpreted in the context of the above reasons as the attenuation of the radiation emitted by the expelled jet material spreading in the space where a powerful explosion of the central engine has swept out the interstellar gas.

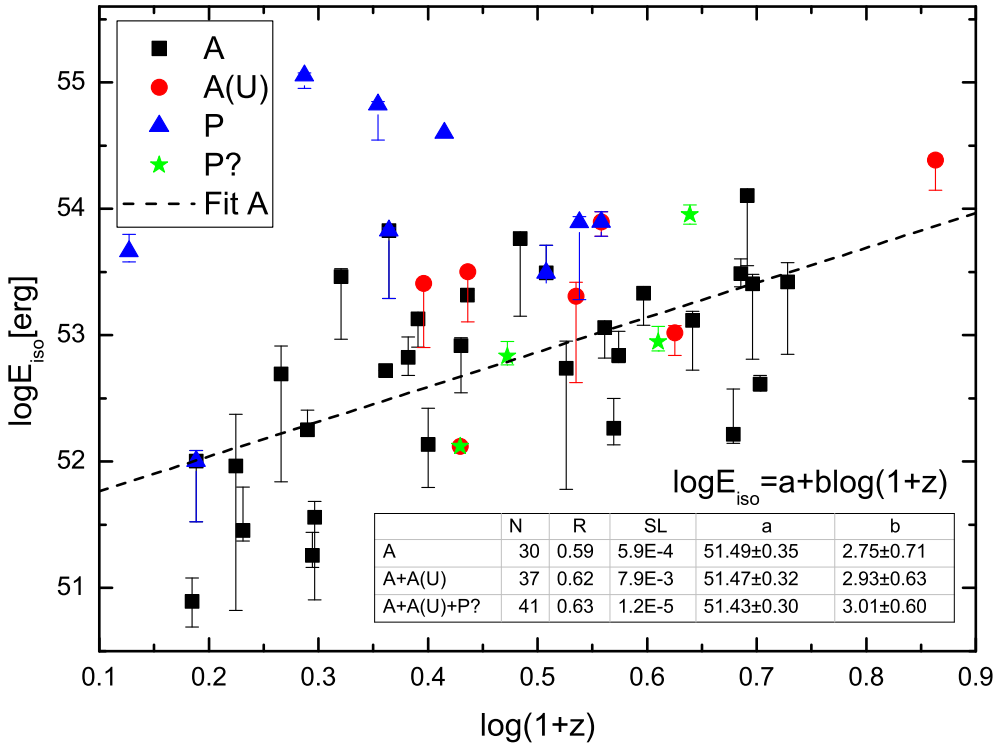

	N	R	SL	a	b
A	30	0.59	5.9E-4	51.49±0.35	2.75±0.71
A+A(U)	37	0.62	7.9E-3	51.47±0.32	2.93±0.63
A+A(U)+P?	41	0.63	1.2E-5	51.43±0.30	3.01±0.60

Figure 3: Dependence of $E_{\rm iso}$ on redshift z.

With great probability the L_R:$(z+1)$ correlation for afterglows is related to the evolution of the density of the local interstellar medium, the regions of active star formation in the host galaxies of gamma-ray bursts, on scales of $0 < z < 6$. The density of interstellar medium determines the character of deceleration of the front shock wave responsible for the late optical emission, namely, the luminosity in the denser media is higher [28].

The absence of peaked afterglows in some of powerful GRBs accompanied by the prompt optical emission is, apparently, evidence of certain differences in their physical natures compared to the other events, especially as, their luminosities do not correlate with redshifts (they drop out of the discovered dependencies). In combination with the fact that the other prompt optical emissions (two orders of magnitude lower by the isotropic equivalent of optical energy E_R) do not alter the correlations obtained, this leads to the idea of specific high-energy sources of gamma-ray bursts, not "feeling" the interstellar medium. On the other hand, it can be assumed that there are sometimes prompt optical emissions

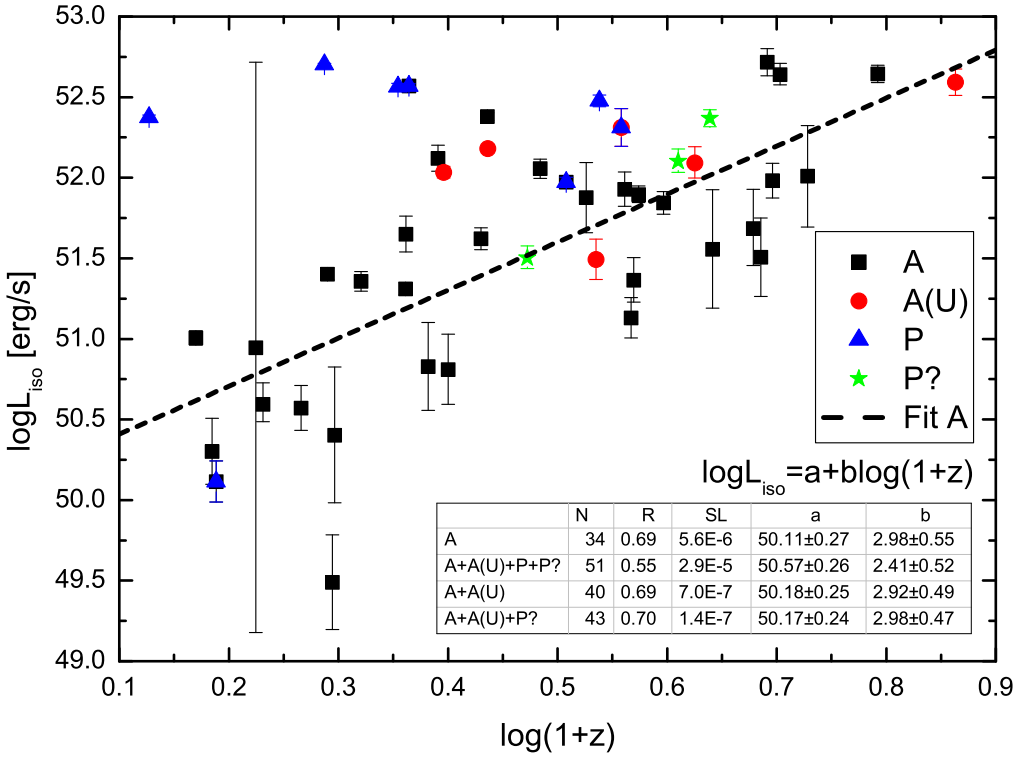

Figure 4: Dependence of $L_{\rm iso}$ on redshift z.

and even gamma-ray emissions (!), susceptible to the interstellar medium during and shortly after the explosion of the central engine.

4 $L_R : E_{\rm iso}$ CORRELATION

We have found the correlation between the luminosity at the optical brightness peak and the energy of gamma-ray radiation almost for all the transient samples (Fig. 5). In particular, for the afterglows (A) it has the form of $L_R \propto E_{\rm iso}^{1.06\pm0.22}$, almost coinciding with the dependence $L_R^{\rm peak} \propto E_{\rm iso}^{1.00\pm0.14}$, earlier obtained in [29]. Such a ratio is typical in the models of deceleration of the front shock wave in the interstellar medium. Let us analyze to what variant of this process does our result correspond.

Consider two regions of the synchrotron spectrum in which the peak of the optical brightness curve can be located [30]. If the characteristic radiation frequency is lower than the characteristic electron cooling frequency $\nu_i < \nu_c$, then the optical spectral index $\beta = \dfrac{p-1}{2}$, where p is the spectral index of emitting electrons $N \propto \epsilon^{-p}$, $2 < p < 3$ [31], and $0.5 < \beta < 1$; yet if $\nu_i > \nu_c$, then $\beta = \dfrac{p}{2}$ and $1 < \beta < 1.5$. At the same time, the observations give $\beta < 1$ [18] with the mean $\beta = 0.75$, whence it follows that the radiation frequency is lower than the frequency of cooling. Let us now analyze the $L_{\rm peak} \propto E_{\rm iso}^{\delta}$ correlation for this case, i.e., at $\nu_i < \nu_c$ [32].

(1) When the energy of both the forward and reverse shock waves is emitted in the optically thin

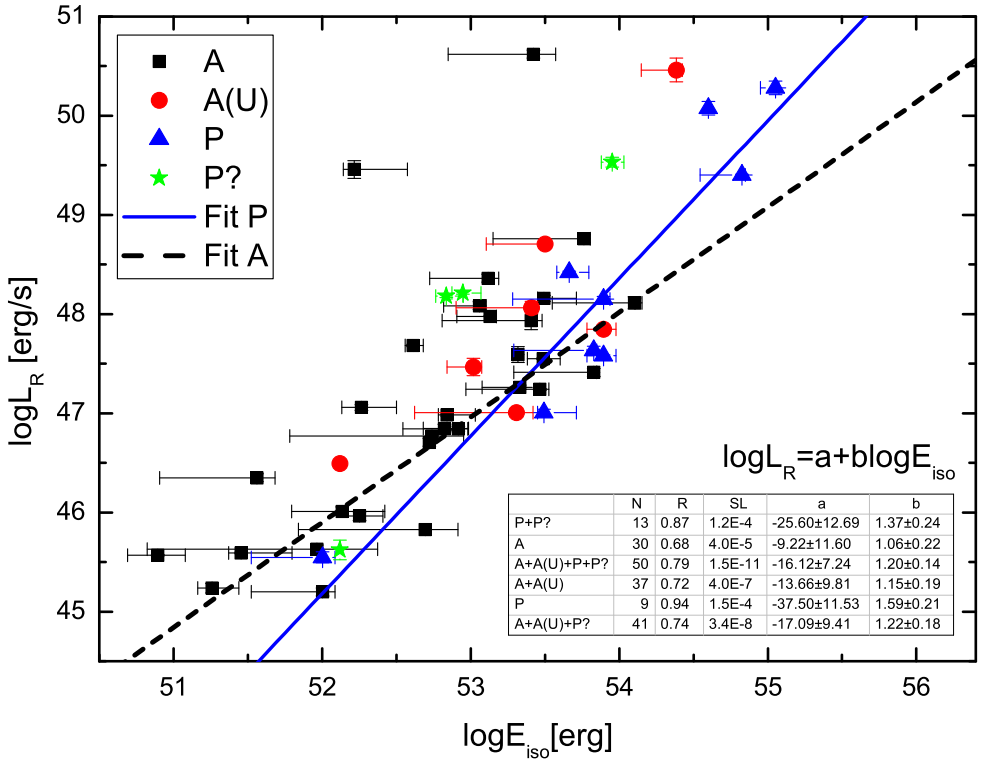

	N	R	SL	a	b
P+P?	13	0.87	1.2E-4	-25.60±12.69	1.37±0.24
A	30	0.68	4.0E-5	-9.22±11.60	1.06±0.22
A+A(U)+P+P?	50	0.79	1.5E-11	-16.12±7.24	1.20±0.14
A+A(U)	37	0.72	4.0E-7	-13.66±9.81	1.15±0.19
P	9	0.94	1.5E-4	-37.50±11.53	1.59±0.21
A+A(U)+P?	41	0.74	3.4E-8	-17.09±9.41	1.22±0.18

Figure 5: Dependence of the R band peak optical luminosity L_R on $E_{\rm iso}$.

plasma, $L_{\rm peak} \propto E_{\rm iso}^{\frac{12-7k-pk}{4(3-k)}}$ and the density profile of the interstellar medium has the form of $n \propto r^{-k}$.

(2) For the optically thick plasma we have:

(a) in the dominance of the forward shock wave, $L_{\rm peak} \propto E_{\rm iso}^{\frac{12-5k+4p-pk}{4(4-k)}}$;

(b) in the dominance of the reverse shock wave, $L_{\rm peak} \propto E_{\rm iso}^{\frac{20-5k-pk}{4(4-k)}}$.

To determine δ, let us use the $0 < k < 1.5$ and $2 < p < 3.5$ estimates obtained in [29]

Given the optically thin plasma, the linear dependence of luminosity on energy ($\delta = 1$), which is close to that we have obtained, can be realized only by the propagation of shock waves in a homogeneous environment, whereas the possibility of its existence around a gamma-ray burst seems improbable. Given the optically thick plasma, the limits on δ both for the forward $0.95 < \delta < 1.625$ and the reverse $0.725 < \delta < 2.5$ shocks are consistent with our estimate. Thus, this analysis shows that the afterglow radiation in the GRB sample with peaked optical light curves can be related both to the forward and reverse shock waves. Notice that the parameters of the linear regression $L_R : E_{\rm iso}$ for the transients from all the samples are very similar within the errors (see Fig. 4). To refine this result, we present in Fig. 6 the dependence of the coefficient of transformation of mechanical energy into optical $\kappa = L_R/E_{\rm iso}$ on the gamma-ray energy. It is clear that this ratio depends both on the actual efficiency coefficient of the conversion of the mechanical energy of the burst into radiation and on the opening angle of the jet. It is easy to see that the behavior of this characteristic is very similar for different transients. It may give evidence on the existence of a relation between the real conversion coefficient

and the opening angle of the jet, which permits equal κ in the regions where the radiation of prompt emissions and afterglows is generated, i.e., at different distances from the central engine.

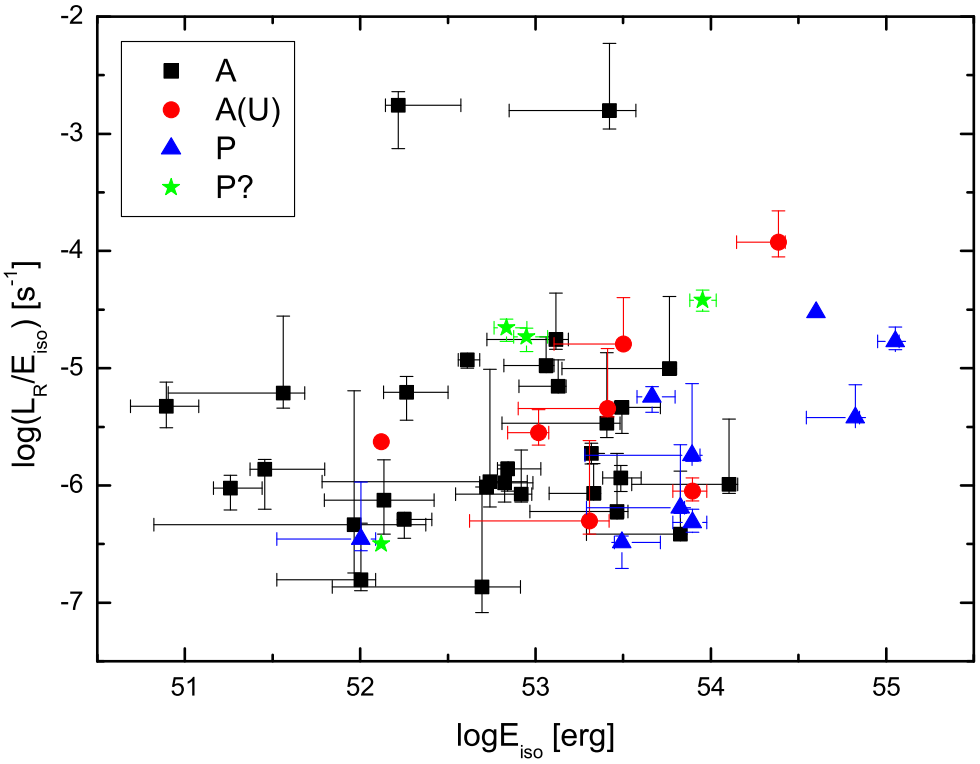

Figure 6: Dependence of the $L_R/E_{\rm iso}$ ratio on $E_{\rm iso}$.

5 $L_R : T_{\rm peak}$ CORRELATION

The study of the character of the correlation between the normalized optical flux and the time of the peak relative to the time of GRB detection $F_{z=z_0} \propto t_{\rm peak}^{-\gamma}$ may clarify various aspects of the physical nature of these objects. Such studies as [33, 21] are devoted to the analysis of this correlation. We believe that a significant disadvantage of these studies is that the examined transients were not divided by their possible origin: prompt emissions, afterglows, and very late emissions were not identified.

In particular, in the latter case, when the peak is reached at $T_{\rm peak} > 10^4$ s, increasing brightness on such time scales is due to the inhomogeneities of the interstellar medium in the propagation of the front shock wave [34], in contrast to the nature of the peaks of prompt emissions and afterglows. In our sample, we have observed an anticorrelation between the optical luminosity at the peak and the time of the peak; however, only for the prompt emissions (P + P?) this correlation is characterized by $\gamma = 3.85 \pm 1.22$ (Fig. 7). The studies [33] and [21] found that $\gamma = 2$ for all the peaked light curves and $\gamma = 1$ for the light curves with a flat region. It appears that this result is of random nature, caused by the presence of prompt emissions in the sample, for which the "luminosity–time of the peak" relationship is indeed valid, as well as several weak late emissions, creating the long-base effect. Let us prove this. Figure 8 demonstrates the points of the $F_{z=2} : t_{\rm peak}$ diagram from [21], divided according to our classification . The Pearson correlation coefficient for all transients from [21] $R = -0.77$, but if

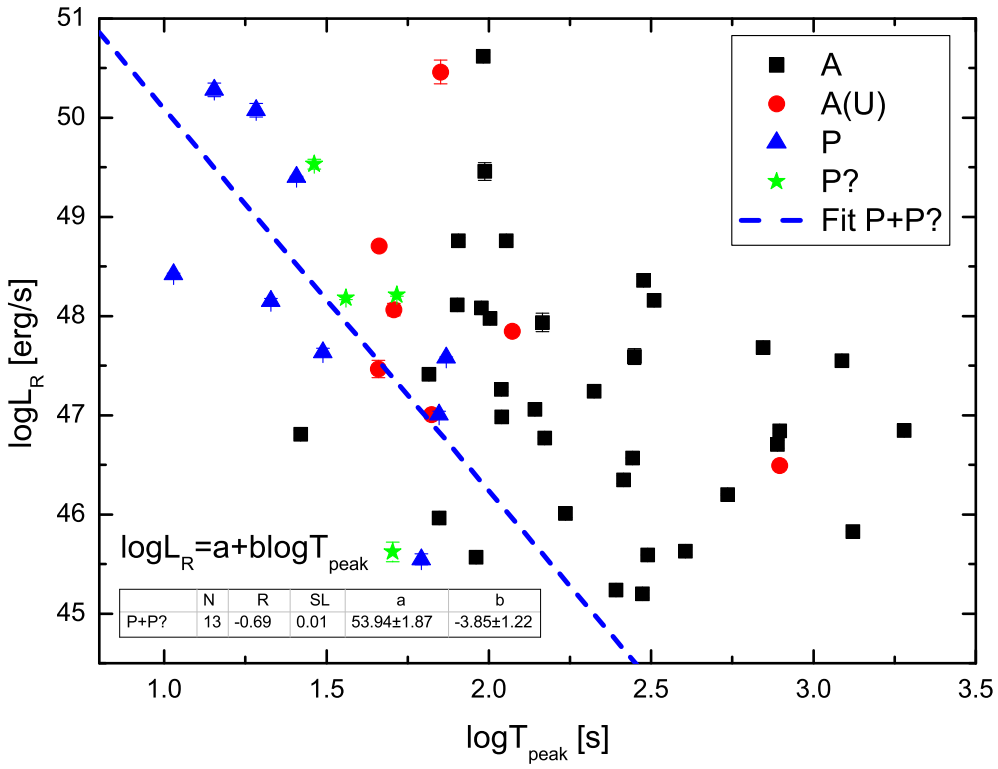

Figure 7: Dependence of the R band peak optical luminosity L_R on the time of the peak $T_{\rm peak}$.

we exclude the P and P?-type emissions, as well as emissions with $t_{\rm peak} > 10^4$ s from this sample, the correlation disappears ($R = -0.44$). To compare our sample with the sample of Panaitescu et al. [21], we have also included the data that the latter work lacked, which further strengthen the assertion about the absence of this correlation for afterglows.

The empirical correlation that we found between the peak luminosity and the time of the peak for the prompt emissions can be interpreted within the model of multiple collisions of plasma ejecta [2]: every event of such a collision generates a single peak, one or a few of which we observe. This process may have a relaxing character: the subsequent warming up events in the collisions of the emitting plasma are less energetic, which qualitatively explains the $L_R \propto T_{\rm peak}^{-3.85\pm1.22}$ correlation that we have found.

6 CONCLUSION

The number of gamma-ray bursts observed to date is great, but we are still very far from getting a thorough understanding of the nature of this phenomenon. In our work we attempted to reveal new properties of gamma-ray bursts with optical components. The results of the study can be briefly summarized as follows.

- Pair correlations between the parameters of gamma-ray bursts in the observed and proper reference frames have been studied, and the statistically significant cases have been identified.
- A correlation has been found, free from selection effects, between the peak luminosity in the

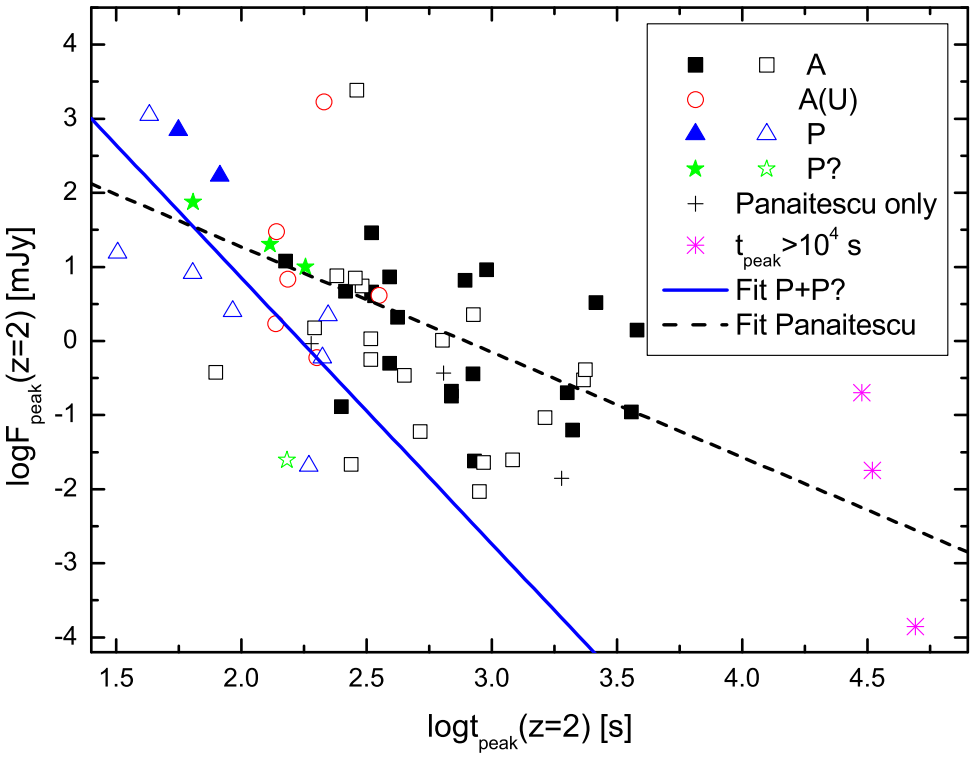

Figure 8: Dependence of the peak flux at $z = 2$ on the time of the peak. The filled symbols mark the data common between our work and Panaitescu et al. [21]; the empty symbols represent the data included in our work and absent in [21]; the crosses denote the data missing in our paper and included in [21] (the asterisks are the objects with $t_{\rm peak} > 10^4$ s).

standard R band and the redshift.

- A step was made to rethink the previously found correlation between the peak luminosity and the time of the peak in the optical light curve: we demonstrate that such a correlation is typical only for prompt optical emissions.
- A hypothesis has been put forward on the presence of a correlation between the efficiency of conversion of the mechanical energy of the relativistic jet into optical radiation and the jet opening angle, providing the similarity of the correlations of optical luminosity and gamma-ray energy for sources differently localized in the jet.

Acknowledgments

The work was partially supported by the grant allocated under the Russian Government Program of Competitive Growth of Kazan Federal University. The study of the statistical properties of gamma-ray bursts as the events contributing to the formation of stellar-planetary associations was supported by the Russian Science Foundation (project 14-50-00043, the Exoplanets program).

Table 2: Parameters of gamma-ray bursts in the observer's frame of reference

GRB	z	$Sample$	t_{peak}	$logF_{opt}$	$logS_{opt}$	α_r	α_d	$logF_{iso}$	$logS_{iso}$
			s	$erg/s\ cm^2$	erg/cm^2			$erg/s\ cm^2$	erg/cm^2
130427A	0.340	P	14.31	-8.21 ± 0.01	-6.80 ± 0.04	1.43	-1.69 ± 0.27	-4.20 ± 0.01	-3.14 ± 0.01
130831A	0.479	A	804.04	-10.83 ± 0.01	-7.96 ± 0.01	0.58	-0.19	$-5.93^{+0.04}_{-0.04}$	-5.05 ± 0.01
081007	0.530	A	139.80	-11.59 ± 0.01	-8.68 ± 0.03	1.04 ± 0.11	-1.14 ± 0.05	$-6.74^{+0.21}_{-0.20}$	-6.23 ± 0.04
060729	0.543	P	95.60	-11.63 ± 0.06	-10.17 ± 0.08	6.72	-3.51 ± 0.80	-6.95 ± 0.13	$-5.39^{+0.04}_{-0.03}$
060729	0.543	A	458.80	-11.97 ± 0.04	-8.64 ± 0.05	0.80 ± 0.12	-0.21 ± 0.04	$-6.95^{+0.13}_{-0.13}$	$-5.39^{+0.04}_{-0.03}$
111209A	0.677	A	676.08	-11.82 ± 0.04				-6.35 ± 1.77	$-5.88^{+0.12}_{-0.13}$
060904B	0.703	A	526.00	-11.97 ± 0.01	-7.93 ± 0.02	0.79 ± 0.5	-1.07 ± 0.06	$-6.74^{+0.13}_{-0.11}$	$-5.73^{+0.09}_{-0.07}$
080710	0.845	A	2441.00	-11.91	-8.12	1.08 ± 0.5	-0.54 ± 0.01	-6.97 ± 0.14	-5.49 ± 0.07
080319B	0.937	P	27.65	-7.55 ± 0.07	-6.08 ± 0.04	2.85 ± 0.54	-4.28 ± 0.34	-4.95 ± 0.01	-3.39 ± 0.01
071010B	0.950	A	136.99	-11.88 ± 0.04	-9.76 ± 0.05	0.62 ± 0.11	-0.38 ± 0.18	$-6.26^{+0.04}_{-0.03}$	-5.29 ± 0.02
070419A	0.971	A	485.82	-12.56 ± 0.05	-9.10 ± 0.07	1.93 ± 0.28	-0.53 ± 0.06	-8.20 ± 0.29	-6.27 ± 0.05
071010A	0.980	A	514.15	-11.50 ± 0.04	-7.53 ± 0.03	0.87 ± 0.09	-0.76 ± 0.01	-7.29 ± 0.42	-6.33 ± 0.09
091024	1.092	A	442.00	-10.78 ± 0.01	-6.98 ± 0.04	1.83 ± 0.05	-1.13 ± 0.06	-6.46 ± 0.06	-4.88 ± 0.02
061007	1.262	P	57.90	-8.92 ± 0.01	-7.22 ± 0.01	5.84 ± 1.89	-1.52 ± 0.08	-5.40 ± 0.02	-3.94 ± 0.01
130420A	1.297	A	1778.28	-11.53 ± 0.04				-6.69 ± 0.04	-5.11
090530	1.300	A	60.48	-11.44 ± 0.04	-7.90 ± 0.05	0.90	-0.68 ± 0.05	-6.35 ± 0.11	-5.73 ± 0.04
061121	1.315	P	71.26	-10.61 ± 0.04	-8.98 ± 0.04	1.83 ± 0.04	-3.24 ± 0.15	-5.44 ± 0.01	-4.55 ± 0.01
061121	1.315	A	151.20	-10.84 ± 0.04	-6.96 ± 0.04	1.44	-1.05 ± 0.01	-5.44 ± 0.01	-4.55 ± 0.01
100901A	1.410	A	4579.20	-11.50 ± 0.04	-6.69 ± 0.03			-7.26 ± 0.27	-5.47 ± 0.06
110213A	1.460	A	248.00	-10.43	-6.14 ± 0.01	0.80	-0.59 ± 0.05	-6.00 ± 0.08	-5.06 ± 0.03
060418	1.489	$A(U)$	127.00	-10.33 ± 0.06	-7.51 ± 0.05	2.28 ± 0.33	-1.13 ± 0.12	-6.11 ± 0.04	-4.88 ± 0.01
080330	1.512	A	432.90	-12.29 ± 0.04	-8.37 ± 0.02			-7.36 ± 0.22	-6.36 ± 0.08
990123	1.600	P	49.88	-8.43 ± 0.07	-6.75 ± 0.07	3.72	-2.37 ± 0.05		-3.21
080603A	1.687	P?	136.00	-13.07 ± 0.10	-11.38 ± 0.12	1.17	-4.26		-5.73
080603A	1.687	$A(U)$	2112.00	-12.20 ± 0.01	-8.05 ± 0.03	0.04 ± 0.01	-0.54 ± 0.11		-5.73
080928	1.692	A	2117.84	-11.80 ± 0.02	-7.88 ± 0.03	2.20 ± 0.68	-0.11 ± 0.02	-6.66 ± 0.07	-5.40 ± 0.03

120119A	1.728	A	766.80	-11.02 ± 0.08	-7.56 ± 0.06	0.44 ± 0.06	-0.65 ± 0.06	-5.93 ± 0.02	-4.63 ± 0.02
100906A	1.730	$A(U)$	125.35	-9.95 ± 0.01	-7.38 ± 0.01	0.46	-0.47 ± 0.06	-6.12 ± 0.02	-4.86 ± 0.01
081008	1.968	P?	107.63	-10.66 ± 0.01	-7.80 ± 0.03	1.26 ± 0.13	-0.72 ± 0.03	$-6.94^{+0.08}_{-0.07}$	$-5.25^{+0.05}_{-0.04}$
081203	2.050	A	345.00	-9.99 ± 0.04	-6.58 ± 0.04	1.18	-1.62 ± 0.05	-6.43 ± 0.06	-4.87 ± 0.02
110205A	2.220	P	226.00	-11.82 ± 0.03	-9.73 ± 0.07	3.43 ± 0.20	-2.92 ± 0.26	-6.60 ± 0.03	-4.70 ± 0.02
110205A	2.220	A	1040.00	-10.67 ± 0.03	-7.30 ± 0.06	1.36 ± 0.26	-1.58 ± 0.02	-6.60 ± 0.03	-4.70 ± 0.02
120815A	2.359	A	499.50	-12.27 ± 0.01	-8.69 ± 0.01	0.15 ± 0.03	-0.50 ± 0.02	-6.77 ± 0.22	-6.27 ± 0.05
080310	2.427	$A(U)$	228.50	-11.86 ± 0.02	-8.35 ± 0.02	1.53 ± 0.13	-0.65 ± 0.09	$-7.17^{+0.13}_{-0.12}$	-5.57 ± 0.03
090812	2.452	P	73.55	-11.10 ± 0.03	-9.37 ± 0.04	1.03 ± 0.03	-1.10 ± 0.03	-6.20 ± 0.04	-4.93 ± 0.02
050820A	2.615	P	267.44	-11.47 ± 0.01	-9.63 ± 0.03	0.59 ± 0.48	-3.59 ± 0.68	-6.43 ± 0.12	-5.06 ± 0.03
050820A	2.615	$A(U)$	426.83	-11.20 ± 0.01	-7.48 ± 0.03	3.21 ± 0.69	-0.89 ± 0.02	-6.43 ± 0.12	-5.06 ± 0.03
080210	2.641	A	345.60	-10.90 ± 0.04	-7.48 ± 0.04	3.66	-1.36 ± 0.02	-6.83 ± 0.11	-5.56 ± 0.03
071031	2.692	A	1023.80	-12.71	-8.85 ± 0.01	1.27 ± 0.07	-0.19 ± 0.03	$-7.64^{+0.13}_{-0.12}$	-5.96 ± 0.06
090726	2.710	A	514.80	-12.13 ± 0.03	-8.90 ± 0.02	1.03 ± 0.05	-1.48 ± 0.16	$-7.42^{+0.14}_{-0.13}$	$-6.19^{+0.05}_{-0.04}$
091029	2.750	A	410.30	-12.13 ± 0.01	-7.91 ± 0.01	0.47	-0.55 ± 0.01	-6.90 ± 0.05	-5.55 ± 0.03
070411	2.950	A	432.00	-12.04 ± 0.02	-7.68 ± 0.04	0.31 ± 0.12	-0.42 ± 0.30	-7.03 ± 0.07	-5.37 ± 0.02
060607A	3.075	P?	212.04	-11.09 ± 0.01	-8.17 ± 0.02	1.87 ± 0.54	-1.31 ± 0.08	$-6.82^{+0.08}_{-0.07}$	$-5.43^{+0.06}_{-0.05}$
060526	3.221	$A(U)$	192.79	-11.80 ± 0.09	-8.13 ± 0.08	0.43	-0.84 ± 0.12	-6.87 ± 0.10	-5.73 ± 0.06
080810	3.355	P?	126.14	-9.98 ± 0.05	-7.11 ± 0.03		-1.94 ± 0.12	-6.63 ± 0.05	-5.01 ± 0.03
090313	3.380	A	1312.80	-11.11 ± 0.04	-6.98 ± 0.06	1.19 ± 0.15	-1.31 ± 0.13	-7.46 ± 0.37	$-5.67^{+0.07}_{-0.08}$
060605	3.773	A	463.00	-10.38 ± 0.09	-6.83 ± 0.12	0.31 ± 0.08	-0.84 ± 0.04	$-7.44^{+0.24}_{-0.23}$	$-6.25^{+0.07}_{-0.09}$
081029	3.848	A	5936.80	-12.29 ± 0.01	-7.89 ± 0.01	1.83 ± 0.15	-0.67 ± 0.03	-7.66 ± 0.24	-5.48 ± 0.05
060210	3.913	A	393.00	-11.55 ± 0.06	-7.92 ± 0.05	1.15 ± 0.64	-1.11 ± 0.04	-6.46 ± 0.08	-4.85 ± 0.02
050730	3.968	A	726.89	-11.63 ± 0.09	-7.62 ± 0.06	0.88 ± 0.25	-0.86 ± 0.06	-7.20 ± 0.11	-5.59 ± 0.04
060206	4.048	A	3534.00	-12.04 ± 0.01	-7.75 ± 0.01	4.65 ± 0.30	-1.12 ± 0.07	$-6.57^{+0.07}_{-0.06}$	$-5.98^{+0.04}_{-0.03}$
080129	4.350	A	514.59	-9.05 ± 0.04	-4.80 ± 0.04			$-7.26^{+0.32}_{-0.31}$	$-5.72^{+0.06}_{-0.07}$
071025	5.200	A	499.40	-11.54 ± 0.03	-8.14 ± 0.05	0.25 ± 0.02	-0.81 ± 0.13	-6.81 ± 0.05	-4.96 ± 0.01
050904	6.295	$A(U)$	518.40	-10.04 ± 0.12	-6.91 ± 0.02	3.46	-4.09	-7.06 ± 0.08	-4.91 ± 0.02

Table 3: Parameters of gamma-ray bursts in the proper frame of reference

GRB	z	$Sample$	T_{peak}	$logL_R$	$logE_R$	T_{90}	$logL_{iso}$	$logE_{iso}$	α
			s	erg/s	erg	s	erg/s	erg	
130427A	0.340	P	10.68	48.42 ± 0.01	49.71 ± 0.04	242.33 ± 1.87	52.38 ± 0.01	$53.66^{+0.13}_{-0.09}$	0.99 ± 0.08
130831A	0.479	A	543.60	46.20 ± 0.01	48.89 ± 0.01	23.43 ± 0.36	51.00 ± 0.04		0.06 ± 0.05
081007	0.530	A	91.40	45.57 ± 0.01	48.29 ± 0.03	3.63 ± 0.17	$50.30^{+0.21}_{-0.21}$	$50.89^{+0.18}_{-0.20}$	$0.65^{+1.02}_{-0.64}$
060729	0.543	P	61.97	45.55 ± 0.06	47.05 ± 0.10	77.22 ± 0.91	50.11 ± 0.13	$52.00^{+0.08}_{-0.48}$	0.23 ± 0.14
060729	0.543	A	297.38	45.20 ± 0.04	77.22 ± 0.91	50.11 ± 0.13	$52.00^{+0.08}_{-0.48}$	0.23 ± 0.14	
111209A	0.677	A	403.15	45.63 ± 0.04		2.77 ± 0.20	50.95 ± 1.77	$51.97^{+0.41}_{-1.14}$	$0.57^{+0.48}_{-0.49}$
060904B	0.703	A	308.88	45.59 ± 0.01	49.41 ± 0.02	100.44 ± 1.34	$50.59^{+0.13}_{-0.11}$	$51.45^{+0.34}_{-0.08}$	$1.00^{+0.69}_{-0.59}$
080710	0.845	A	1322.75	45.832	49.35	75.35 ± 5.43	50.57 ± 0.14	$52.69^{+0.22}_{-0.85}$	0.74 ± 0.24
080319B	0.937	P	14.27	50.28 ± 0.07	51.47 ± 0.04	76.06 ± 1.29	52.70 ± 0.01	$55.05^{+0.02}_{-0.10}$	0.91 ± 0.02
071010B	0.950	A	70.25	45.96 ± 0.04	47.80 ± 0.05	17.78 ± 0.52	$51.40^{+0.04}_{-0.03}$	$52.25^{+0.16}_{-0.04}$	$0.53^{+0.23}_{-0.22}$
070419A	0.971	A	246.55	45.24 ± 0.05	48.41 ± 0.07	81.83 ± 4.5	49.49 ± 0.29	$51.26^{+0.18}_{-0.10}$	
071010A	0.980	A	259.67	46.35 ± 0.04	50.03 ± 0.03	11.31 ± 0.86	50.40 ± 0.42	$51.56^{+0.12}_{-0.66}$	
091024	1.092	A	211.24	47.24 ± 0.01	50.73 ± 0.04	54.83 ± 2.37	51.36 ± 0.06	$53.46^{+0.06}_{-0.50}$	0.72 ± 0.07
061007	1.262	P	25.59	49.40 ± 0.01	51.07 ± 0.01	33.118 ± 0.23	52.57 ± 0.02	$54.83^{+0.02}_{-0.28}$	1.04 ± 0.03
130420A	1.297	A	774.17	46.71 ± 0.04		50.00 ± 2.11	51.31 ± 0.04	52.72	$0.88^{+0.68}_{-0.41}$
090530	1.300	A	26.30	46.81 ± 0.04	49.99 ± 0.05	17.72 ± 0.50	51.65 ± 0.11		0.43 ± 0.16
061121	1.315	P	30.79	47.64 ± 0.04	48.90 ± 0.04	35.86 ± 5.40	52.57 ± 0.01	$53.83^{+0.02}_{-0.54}$	0.63 ± 0.03
061121	1.315	A	65.33	47.41 ± 0.04	50.92 ± 0.04	35.86 ± 5.40	52.57 ± 0.01	$53.83^{+0.02}_{-0.54}$	0.63 ± 0.03
100901A	1.410	A	1900.08	46.85 ± 0.04	51.27 ± 0.03	190.54 ± 4.42	50.83 ± 0.27	$52.82^{+0.16}_{-0.14}$	$0.45^{+0.22}_{-0.23}$
110213A	1.460	A	100.81	47.98	51.87 ± 0.01	17.53 ± 1.41	52.12 ± 0.08	$53.13^{+0.04}_{-0.22}$	0.18 ± 11
060418	1.489	$A(U)$	51.02	48.07 ± 0.06	50.49 ± 0.05	41.48 ± 4.15	52.03 ± 0.04	$53.41^{+0.03}_{-0.51}$	0.39 ± 0.05
080330	1.512	A	172.34	46.01 ± 0.04	49.53 ± 0.02	26.31 ± 0.39	50.81 ± 0.22	$52.14^{+0.29}_{-0.34}$	
990123	1.600	P	19.18	50.08 ± 0.07	51.15 ± 0.07			54.60	
080603A	1.687	P?	50.61	45.62 ± 0.10	48.16 ± 0.05			52.12	
080603A	1.687	$A(U)$	785.89	46.49 ± 0.01	50.20 ± 0.03			52.12	
080928	1.692	A	786.72	46.84 ± 0.02	50.33 ± 0.03	105.83 ± 4.52	51.62 ± 0.07	$52.92^{+0.06}_{-0.37}$	$0.27^{+0.12}_{-0.13}$

120119A	1.728	A	281.09	47.59 ± 0.08	50.61 ± 0.06	25.81 ± 1.59	52.38 ± 0.02	$53.32^{+0.04}_{-0.03}$	$0.95^{+0.14}_{-0.13}$
100906A	1.730	$A(U)$	45.92	48.71 ± 0.01	50.82 ± 0.01	42.80 ± 0.25	52.18 ± 0.02	$53.50^{+0.02}_{-0.40}$	0.34 ± 0.04
081008	1.968	P?	36.26	48.18 ± 0.01	49.70 ± 0.01	67.15 ± 3.88	$51.50^{+0.08}_{-0.07}$	$52.83^{+0.11}_{-0.07}$	$0.70^{+0.34}_{-0.31}$
081203	2.050	A	113.11	48.76 ± 0.04	51.69 ± 0.04	83.37 ± 8.83	52.06 ± 0.06	$53.76^{+0.04}_{-0.61}$	0.56 ± 0.06
110205A	2.220	P	70.19	47.01 ± 0.03	48.59 ± 0.07	86.03 ± 1.45	51.97 ± 0.03	$53.49^{+0.22}_{-0.04}$	$0.61^{+0.18}_{-0.17}$
110205A	2.220	A	322.98	48.16 ± 0.03	51.02 ± 0.04	86.03 ± 1.45	51.97 ± 0.03	$53.49^{+0.22}_{-0.04}$	$0.61^{+0.18}_{-0.17}$
120815A	2.359	A	148.72	46.77 ± 0.01	49.83 ± 0.01	2.88 ± 0.36	51.88 ± 0.22	$52.74^{+0.21}_{-0.96}$	
080310	2.427	$A(U)$	66.67	47.01 ± 0.02	49.98 ± 0.02	105.60 ± 1.10	$51.49^{+0.13}_{-0.12}$	$53.31^{+0.11}_{-0.68}$	
090812	2.452	P	21.31	48.15 ± 0.03	49.50 ± 0.04	28.90 ± 4.43	52.48 ± 0.04	$53.89^{+0.04}_{-0.61}$	0.71 ± 0.06
050820A	2.615	P	73.99	47.58 ± 0.01	49.15 ± 0.02	66.31 ± 0.10	52.31 ± 0.12	$53.89^{+0.08}_{-0.11}$	0.83 ± 0.11
050820A	2.615	$A(U)$	118.08	47.85 ± 0.02	51.06 ± 0.02	66.31 ± 0.10	52.31 ± 0.12	$53.89^{+0.08}_{-0.11}$	0.83 ± 0.11
080210	2.641	A	94.92	48.08 ± 0.04	50.73 ± 0.04	12.05 ± 1.20	51.93 ± 0.11	$53.06^{+0.05}_{-0.24}$	0.25 ± 0.12
071031	2.692	A	277.30	46.57	49.87 ± 0.01	50.70 ± 1.93	$51.13^{+0.13}_{-0.12}$		
090726	2.710	A	138.76	47.06 ± 0.03	49.72 ± 0.02	13.75 ± 0.26	$51.36^{+0.14}_{-0.13}$	$52.26^{+0.24}_{-0.13}$	
091029	2.750	A	109.41	46.98 ± 0.01	50.63 ± 0.01	10.66 ± 0.34	51.89 ± 0.05	$52.84^{+0.19}_{-0.06}$	$0.60^{+0.32}_{-0.30}$
070411	2.950	A	109.37	47.26 ± 0.02	51.02 ± 0.02	27.48 ± 0.92	51.84	$53.33^{+0.04}_{-0.25}$	0.30 ± 0.10
060607A	3.075	P?	52.04	48.21 ± 0.01	50.52 ± 0.02	25.17 ± 0.82	$52.10^{+0.08}_{-0.07}$	$52.95^{+0.12}_{-0.07}$	$0.99^{+0.32}_{-0.34}$
060526	3.221	$A(U)$	45.67	47.47 ± 0.09	50.51 ± 0.08	70.01 ± 0.95	52.09 ± 0.10	$53.02^{+0.06}_{-0.18}$	
080810	3.355	P?	28.97	49.53 ± 0.05	51.76 ± 0.03	104.05 ± 1.17	52.37 ± 0.05	$53.95^{+0.08}_{-0.07}$	0.69 ± 0.12
090313	3.380	A	299.73	48.36 ± 0.04	51.85 ± 0.06	20.60 ± 1.54	51.56 ± 0.37	$53.12^{+0.07}_{-0.39}$	
060605	3.773	A	97.00	49.46 ± 0.09	52.33 ± 0.12	3.88 ± 0.24	$51.69^{+0.24}_{-0.23}$	$52.22^{+0.36}_{-0.07}$	
081029	3.848	A	1224.61	47.55 ± 0.01	51.26 ± 0.01	34.88 ± 1.76	51.51 ± 0.24	$53.49^{+0.12}_{-0.10}$	0.57 ± 0.20
060210	3.913	A	79.99	48.11 ± 0.06	51.05 ± 0.05	75.30 ± 4.20	52.72 ± 0.08	$54.10^{+0.05}_{-0.56}$	0.53 ± 0.10
050730	3.968	A	146.31	47.94 ± 0.09	50.85 ± 0.06	12.17 ± 0.45	51.98 ± 0.11	$53.41^{+0.08}_{-0.60}$	0.61 ± 0.13
060206	4.048	A	700.08	47.68 ± 0.01	51.27 ± 0.01	1.20 ± 0.03	$52.64^{+0.07}_{-0.06}$	$52.61^{+0.07}_{-0.05}$	$0.82^{+0.33}_{-0.31}$
080129	4.350	A	96.18	50.62 ± 0.04	54.14 ± 0.04	8.52 ± 0.56	$52.01^{+0.32}_{-0.31}$	$53.42^{+0.15}_{-0.57}$	$0.78^{+0.253}_{-0.24}$
071025	5.200	A	80.55	48.76 ± 0.03	51.36 ± 0.05	26.00 ± 0.87	52.64 ± 0.05		0.33 ± 0.06
050904	6.295	$A(U)$	71.06	50.46 ± 0.12	52.73 ± 0.12	27.03 ± 0.31	52.59 ± 0.08	$54.38^{+0.04}_{-0.24}$	0.83 ± 0.07

Table 4: Pair correlations between gamma-ray burst parameters with correlation coefficients $R > 0.5$ and significance levels SL $< 1\%$. The table lists the linear regression parameters $(a + bx)$ (the variables are given in the logarithmic scale)

Correlation	Sample	N	R	SL	a	b
	P+P?	11	0.86	$0.72 \cdot 10^{-3}$	-19.44 ± 16.25	1.40 ± 0.31
	A	30	0.80	$0.91 \cdot 10^{-7}$	11.00 ± 5.85	0.81 ± 0.11
$E_{iso} - L_{iso}$	A+A(U)+P+P?	47	0.84	$0.11 \cdot 10^{-12}$	4.37 ± 4.64	0.94 ± 0.09
	P	8	0.89	$0.32 \cdot 10^{-2}$	3.29 ± 10.67	0.97 ± 0.20
	A+A(U)	36	0.82	$0.86 \cdot 10^{-9}$	8.32 ± 5.31	0.86 ± 0.10
	A+A(U)+P?	39	0.82	$0.13 \cdot 10^{-10}$	8.10 ± 5.09	0.87 ± 0.10
	P+P?	13	0.95	$0.51 \cdot 10^{-6}$	6.81 ± 4.14	0.89 ± 0.09
	A	32	0.92	$0.42 \cdot 10^{-13}$	3.82 ± 3.51	0.99 ± 0.07
	A(U)	7	0.92	$0.29 \cdot 10^{-2}$	19.67 ± 5.76	0.65 ± 0.12
$E_R - L_R$	A+A(U)+P+P?	52	0.80	$0.92 \cdot 10^{-12}$	13.13 ± 3.92	0.78 ± 0.08
	A+A(U)	39	0.91	$0.89 \cdot 10^{-15}$	7.80 ± 3.10	0.90 ± 0.07
	P	9	0.99	$0.11 \cdot 10^{-6}$	4.74 ± 2.06	0.93 ± 0.04
	A+A(U)+P?	43	0.89	$0.13 \cdot 10^{-14}$	9.02 ± 3.31	0.87 ± 0.04
	P+P?	13	0.76	$0.25 \cdot 10^{-2}$	-10.75 ± 15.56	1.13 ± 0.29
	A	32	0.65	$0.16 \cdot 10^{-3}$	-7.39 ± 13.13	1.10 ± 0.50
$E_R - E_{iso}$	A+A(U)+P+P?	48	0.52	$0.14 \cdot 10^{-3}$	-9.10 ± 9.95	0.78 ± 0.19
	A+A(U)	35	0.66	$0.15 \cdot 10^{-4}$	-4.02 ± 10.79	1.03 ± 0.20
	P	9	0.96	$0.42 \cdot 10^{-4}$	-32.27 ± 9.07	1.52 ± 0.17
	A+A(U)+P?	39	0.68	$0.22 \cdot 10^{-5}$	-7.07 ± 10.29	1.09 ± 0.19
	A	34	0.79	$0.30 \cdot 10^{-7}$	44.68 ± 0.37	5.39 ± 0.74
$L_R - z + 1$	A+A(U)+P+P?	54	0.56	$0.13 \cdot 10^{-4}$	45.48 ± 0.45	4.36 ± 0.90
	A+A(U)	41	0.78	$0.19 \cdot 10^{-8}$	44.67 ± 0.36	5.54 ± 0.71
	A+A(U)+P?	45	0.77	$0.54 \cdot 10^{-9}$	44.58 ± 0.37	5.57 ± 0.72
	A	32	0.65	$0.65 \cdot 10^{-4}$	-4.92 ± 11.95	1.07 ± 0.23
$E_R - L_{iso}$	A+A(U)+P+P?	49	0.56	$0.30 \cdot 10^{-4}$	1.76 ± 10.51	0.94 ± 0.20
	A+A(U)	38	0.66	$0.66 \cdot 10^{-5}$	-5.49 ± 10.63	1.09 ± 0.21
	A+A(U)+P?	41	0.66	$0.23 \cdot 10^{-5}$	-5.79 ± 10.17	1.09 ± 0.20
	P+P?	13	0.87	$0.12 \cdot 10^{-3}$	-25.60 ± 12.69	1.37 ± 0.24
	A	30	0.68	$0.40 \cdot 10^{-4}$	-9.22 ± 11.60	1.06 ± 0.22
$L_R - E_{iso}$	A+A(U)+P+P?	50	0.79	$0.15 \cdot 10^{-10}$	-16.12 ± 7.24	1.20 ± 0.14
	A+A(U)	37	0.72	$0.40 \cdot 10^{-6}$	-13.66 ± 9.81	1.15 ± 0.19
	P	9	0.94	$0.15 \cdot 10^{-3}$	-37.50 ± 11.53	1.59 ± 0.21
	A+A(U)+P?	41	0.74	$0.34 \cdot 10^{-7}$	-17.09 ± 9.41	1.22 ± 0.18
	A	34	0.74	$0.51 \cdot 10^{-6}$	-13.49 ± 9.60	1.18 ± 0.19
$L_R - L_{iso}$	A+A(U)+P+P?	51	0.78	$0.21 \cdot 10^{-10}$	-20.33 ± 7.80	1.31 ± 0.15
	A+A(U)	40	0.76	$0.14 \cdot 10^{-7}$	-18.38 ± 9.10	1.27 ± 0.18
	A+A(U)+P?	43	0.76	$0.30 \cdot 10^{-8}$	-20.36 ± 8.90	1.31 ± 0.18
	A	30	0.59	$0.59 \cdot 10^{-3}$	51.49 ± 0.35	2.75 ± 0.71
$E_{iso} - z + 1$	A+A(U)	37	0.62	$0.79 \cdot 10^{-2}$	51.47 ± 0.32	2.93 ± 0.63
	A+A(U)+P?	41	0.63	$0.12 \cdot 10^{-4}$	51.43 ± 0.30	3.01 ± 0.60
$L_R - Tpeak$	P+P?	13	-0.69	0.01	53.94 ± 1.87	-3.85 ± 1.22
	A	32	0.72	$0.34 \cdot 10^{-5}$	47.97 ± 0.47	5.29 ± 0.93
$E_{opt} - z + 1$	A+A(U)+P+P?	52	0.63	$0.50 \cdot 10^{-6}$	48.06 ± 0.42	4.84 ± 0.84

	A+A(U)	39	0.73	$0.12 \cdot 10^{-6}$	48.01 ± 0.41	5.18 ± 0.79
	A+A(U)+P?	43	0.71	$0.76 \cdot 10^{-7}$	47.89 ± 0.42	5.28 ± 0.84
	A	34	0.69	$0.56 \cdot 10^{-5}$	50.11 ± 0.27	2.98 ± 0.55
$L_{iso} - z + 1$	A+A(U)+P+P?	51	0.55	$0.29 \cdot 10^{-4}$	50.57 ± 0.26	2.41 ± 0.52
	A+A(U)	40	0.69	$0.70 \cdot 10^{-6}$	50.18 ± 0.25	2.92 ± 0.49
	A+A(U)+P?	43	0.70	$0.14 \cdot 10^{-6}$	50.17 ± 0.24	2.98 ± 0.47

References

[1] P. Mészáros and M. J. Rees, ApJ **476**, 232 (1997).

[2] M. J. Rees and P. Meszaros, ApJ **430**, L93 (1994).

[3] N. Gehrels and S. Razzaque, Frontiers of Physics **8**, 661 (2013).

[4] J. P. Norris, G. F. Marani, and J. T. Bonnell, ApJ **534**, 248 (2000).

[5] L. Borgonovo and F. Ryde, ApJ **548**, 770 (2001).

[6] L. Amati, F. Frontera, M. Tavani, et al., A&A **390**, 81 (2002).

[7] C. Guidorzi, F. Frontera, E. Montanari, et al., MNRAS **363**, 315 (2005).

[8] G. Ghirlanda, G. Ghisellini, C. Firmani, et al., MNRAS **360**, L45 (2005).

[9] G. Ghirlanda, G. Ghisellini, and C. Firmani, New J. Physics **8**, 123 (2006).

[10] L.-X. Li and B. Paczyński, MNRAS **366**, 219 (2006).

[11] A. Zeh, S. Klose, and D. A. Kann, ApJ **637**, 889 (2006).

[12] M. Nardini, G. Ghisellini, G. Ghirlanda, et al., A&A **451**, 821 (2006).

[13] D. A. Kann, S. Klose, B. Zhang, et al., ApJ **720**, 1513 (2010).

[14] L. Li, E.-W. Liang, Q.-W. Tang, et al., ApJ **758**, 27 (2012).

[15] E. Zaninoni, M. G. Bernardini, R. Margutti, et al., A&A **557**, A12 (2013).

[16] A. Melandri, S. Covino, D. Rogantini, et al., A&A **565**, A72 (2014).

[17] P. Schady, T. Dwelly, M. J. Page, et al., A&A **537**, A15 (2012).

[18] T. Zafar, D. Watson, J. P. U. Fynbo, et al., A&A **532**, A143 (2011).

[19] S. Schulze, S. Klose, G. Björnsson, et al., A&A **526**, A23 (2011).

[20] M. Fukugita, K. Shimasaku, and T. Ichikawa, ASP**107**, 945 (1995).

[21] A. Panaitescu, W. T. Vestrand, and P. Woźniak, MNRAS **433**, 759 (2013).

[22] N. R. Butler, D. Kocevski, J. S. Bloom, and J. L. Curtis, ApJ **671**, 656 (2007).

[23] D. J. Schlegel, D. P. Finkbeiner, and M. Davis, ApJ **500**, 525 (1998).

[24] Y. C. Pei, ApJ **395**, 130 (1992).

[25] D. M. Coward, E. J. Howell, M. Branchesi, et al., MNRAS **432**, 2141 (2013).

[26] G. Beskin, G. Oganesyan, G. Greco, and S. Karpov, EAS Publ. Ser. **61**, 241 (2013).

[27] L.-X. Li, MNRAS **379**, L55 (2007).

[28] L. J. Gou, P. Mészáros, T. Abel, and B. Zhang, ApJ **604**, 508 (2004).

[29] E.-W. Liang, L. Li, H. Gao, et al., ApJ **774**, 13 (2013).

[30] A. Panaitescu, AIP Conf. Ser. **1133**, 127 (2009).

[31] T. Piran, Rev. Modern Physics **76**, 1143 (2004).

[32] H. J. van Eerten, MNRAS **445**, 2414 (2014).

[33] A. Panaitescu and W. T. Vestrand, MNRAS **414**, 3537 (2011).

[34] D. Lazzati, E. Rossi, S. Covino, et al., A&A **396**, L5 (2002).